Membrane chaperone Shr3 assists in folding amino acid permeases preventing precocious ERAD

Jhansi Kota, C. Fredrik Gilstring, and Per O. Ljungdahl

Ludwig Institute for Cancer Research, S-17177 Stockholm, Sweden

The yeast endoplasmic reticulum (ER) membrane-localized chaperone Shr3 plays a critical role in enabling amino acid permeases (AAPs) to fold and attain proper structures required for functional expression at the plasma membrane. In the absence of Shr3, AAPs specifically accumulate in the ER, where despite the correct insertion of their 12 transmembrane segments (TMSs), they aggregate forming large molecular weight complexes. We show that Shr3 prevents aggregation and facilitates the functional assembly of independently co-expressed N- and C-terminal fragments of the general AAP Gap1. Shr3 interacts with and maintains the first five TMSs in a conformation that can posttranslationally assemble with the remaining seven TMSs. We also show that Doa10- and Hrd1-dependent ER-associated degradation (ERAD) pathways redundantly degrade AAP aggregates. In combination, *doa10Δ hrd1Δ* mutations stabilize AAP aggregates and partially suppress amino acid uptake defects of *shr3* mutants. Consequently, in cells with impaired ERAD, AAPs are able to attain functional conformations independent of Shr3. These findings illustrate that folding and degradation are tightly coupled processes during membrane protein biogenesis.

Introduction

Early in the secretory pathway of eukaryotic cells, integral plasma membrane (PM) proteins are inserted into the lipid bilayer of the ER. The mechanisms enabling polytopic membrane proteins, composed of multiple transmembrane segments (TMSs), to integrate and fold in the ER membrane are not well documented. It is known that hydrophobic amino acids within N-terminally localized TMSs are sufficient to target membrane proteins to the ER, where they interact with and enter a protein-conducting channel, or translocon, with a hydrophilic core. The translocon is a highly conserved heterotrimeric integral membrane complex, i.e., the Sec61 complex in eukaryotes and SecY complex in bacteria (Osborne et al., 2005).

The successful ability to crystallize membrane proteins has greatly enhanced the understanding of two basic processes associated with membrane protein biogenesis. First, the structure of the *Methanococcus jannaschii* SecY translocon has been elucidated (van den Berg et al., 2004), which revealed that the protein-conducting channel is contained within SecY, the largest translocon subunit and the Sec61 homologue. Despite unresolved questions regarding the structure of an active Sec61/SecY translocon in vivo (Alder and Johnson, 2004), the protein-conducting channel, although perhaps quite flexible, is too small to accommodate multiple TMSs (Rapoport et al., 2004; Osborne et al., 2005). Second, the structures of bacterial PM transporters LacY and GlpT, each composed of 12 TMSs (Abramson et al., 2003; Huang et al., 2003), have clearly shown that interactions between TMSs within the lipid phase of the membrane are not limited to immediately flanking TMSs. Consequently, to fold properly, N-terminally localized TMSs that partition into the membrane of partially translated proteins must await the insertion of C-terminal TMSs. Together, these advances are consistent with the idea that polytopic membrane protein biogenesis occurs essentially in two discrete stages, i.e., membrane insertion and folding (Popot and Engelman, 1990; Engelman et al., 2003; Bowie, 2005).

To bridge these stages, and to account for the fact that polytopic membrane proteins cannot fold in a strict cotranslational manner, the existence of chaperone-like proteins has been postulated (Lecomte et al., 2003; Alder and Johnson, 2004; Rapoport et al., 2004). The identification of membrane-localized chaperones in bacteria (Nagamori et al., 2004) and yeast

Correspondence to Per O. Ljungdahl: plju@wgi.su.se

P.O. Ljungdahl's present address is Department of Cell Biology, Wenner-Gren Institute, Stockholm University, SE-106 91 Stockholm, Sweden.

Abbreviations used in this paper: AAP, amino acid permease; AzC, analogue azetidine-2-carboxylate; BN-PAGE, blue native PAGE; CFTR, cystic fibrosis transmembrane conductance regulator; DM, dodecyl-β-D-maltopyranoside; ERAD, ER-associated degradation; HMG CoA, 3-hydroxy-3-methylglutaryl coenzyme A; INSIG, insulin-induced gene; PM, plasma membrane; TMS, transmembrane segment.

The Journal of Cell Biology, Vol. 176, No. 5, February 26, 2007 617–628
http://www.jcb.org/cgi/doi/10.1083/jcb.200612100

(Kota and Ljungdahl, 2005) provided strong support for this notion. Consistent with the two-stage model of biogenesis, these chaperones do not appear to be necessary for the insertion of TMSs (Gilstring and Ljungdahl, 2000; Nagamori et al., 2004) but, nonetheless, they appear to interact early during the translocation process to enable their substrate proteins to obtain native conformations (Nagamori et al., 2004; Kota and Ljungdahl, 2005). Although it remains to be determined, this novel class of chaperones may prevent TMSs of polytopic membrane proteins that do not normally interact in the mature protein from engaging in nonproductive interactions with flanking TMSs, or with other ER components, as they sequentially partition into the membrane.

In the yeast *Saccharomyces cerevisiae*, the recently characterized membrane-localized chaperones exhibit a striking degree of substrate specificity. The best studied of these chaperones, Shr3, is specifically required for proper folding of amino acid permeases (AAPs; Kota and Ljungdahl, 2005). AAPs comprise a conserved family of 18 proteins with 12 TMSs (Gilstring and Ljungdahl, 2000). AAPs localize to the PM in an Shr3-dependent manner (Ljungdahl et al., 1992), where they function to transport amino acids into cells. In the absence of Shr3 chaperone activity, AAPs aggregate, forming large molecular weight complexes (Kota and Ljungdahl, 2005), which are excluded from coatomer protein II transport vesicles (Kuehn et al., 1996, 1998). Consequently, AAPs accumulate in the ER of *shr3*-null mutant strains. Shr3 has two well-defined domains, a membrane domain composed of four TMSs and a hydrophilic C-terminal domain. The chaperone activity of Shr3 is associated with the membrane domain; the hydrophilic C-terminal domain is dispensable for function (Kota and Ljungdahl, 2005). The steady-state levels of AAPs are similar in both wild-type and *shr3*-null mutant cells (Ljungdahl et al., 1992; Gilstring et al., 1999; Kota and Ljungdahl, 2005). In wild-type cells, AAPs are degraded in the vacuole (Roberg et al., 1997; Springael and André, 1998); the fate of aggregated AAPs in *shr3* mutants has not been investigated.

PM and secretory proteins are subject to ER quality-control systems that operate to ensure that only properly folded and assembled proteins exit the ER and enter into subsequent stages of the secretory pathway (Ellgaard et al., 1999). The ER lumen contains numerous factors that assist folding reactions (Nishikawa et al., 2005; Bukau et al., 2006). Terminally misfolded, or incompletely assembled soluble or integral membrane proteins are degraded in a process referred to as ER-associated degradation (ERAD; Meusser et al., 2005). ERAD substrates are passed through or extracted from the membrane, ubiquitylated, and ultimately presented to cytoplasmic proteasomes for degradation. Several ERAD pathways have been defined (Huyer et al., 2004; Vashist and Ng, 2004; Ravid et al., 2006). These pathways are composed of multimeric protein complexes organized around two membrane-localized E3 ubiquitin ligases, i.e., Doa10 and Hrd1 (Carvalho et al., 2006; Denic et al., 2006). These pathways appear to differentially recognize ERAD substrates, and thus far, all characterized ERAD substrates exhibit a strong dependence on either Doa10 or Hrd1 pathways. With respect to polytopic membrane proteins, little is known regarding how ERAD surveillance mechanisms differentiate between proteins in the process of membrane insertion and folding from proteins that are terminally misfolded. The potential involvement of membrane-localized chaperones in ERAD has not been examined.

We have investigated the chaperone activity of Shr3 from two perspectives. Using split Gap1 constructs, we examined the temporal requirement of Shr3 during membrane insertion and folding. Our results indicate that Shr3 interacts with an N-terminal fragment composed of TMSs I–V and maintains it in a conformation that enables it to functionally assemble with a coexpressed C-terminal fragment with TMSs VI–XII. Second, we assessed the potential role of Shr3 in quality-control mechanisms that monitor AAP folding. We report that in the absence of Shr3, Gap1 aggregates are redundantly targeted to Doa10- and Hrd1-dependent ERAD pathways. Cells lacking these ERAD pathways exhibit restored amino acid uptake capacities. Thus, given sufficient time, AAPs are able to attain functional conformations independent of Shr3. These findings highlight the intimate link between folding and degradation during the biogenesis of polytopic membrane proteins.

Results

Shr3-dependent localization of Gap1

Previous studies examining the ER retention of AAP in *shr3* mutants have relied on microscopic evaluation (Ljungdahl et al., 1992; Kota and Ljungdahl, 2005). The intracellular distribution of Gap1 in wild-type and *shr3Δ* mutant strains was examined by subcellular fractionation of whole cell lysates. In lysates from wild-type cells (Fig. 1, left) the majority of Gap1 cofractionated with the PM marker protein Pma1 (fractions 2 and 3) and the late Golgi marker Kex2 (peak fraction 6). The distribution of Gap1 was distinct from the ER marker Wbp1, which exhibited the highest concentration in fraction 5. Gap1 migrated as two bands: a top band present in PM-containing fractions and a bottom band that was observed in fractions containing internal membranes. Gap1 is known to be posttranslationally modified by phosphorylation, which correlates with increased amino acid uptake (Stanbrough and Magasanik, 1995). Also, phosphorylation is important for proper targeting of Gap1 from the Golgi to the PM and for preventing Gap1 down-regulation

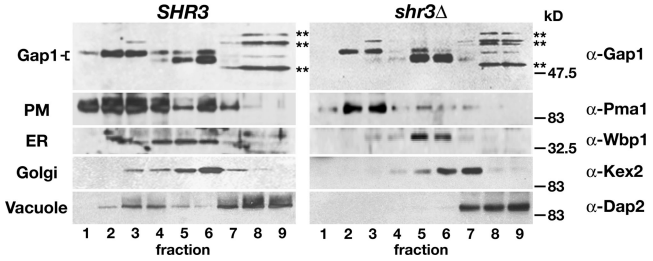

Figure 1. **Gap1 requires Shr3 for proper intracellular localization.** Cell lysates prepared from *SHR3* (PLY127) and *shr3Δ6* (FGY212) cells grown in SUD were fractionated on 12–60% step sucrose gradients. Proteins within fractions were separated by SDS-PAGE and analyzed by immunoblotting. The antibodies recognizing marker proteins Pma1 (100 kD), Wbp1 (49 kD), Kex2 (90 kD), and Dap2 (93 kD) were used to identify fractions containing PM, ER, Golgi, and vacuolar proteins, respectively. The asterisks indicate nonspecific immunoreactive bands unrelated to Gap1.

(De Craene et al., 2001). The pattern of mobility we observed likely correlates with Gap1 becoming phosphorylated as it progresses through the secretory pathway on its way to the PM.

In lysates from *shr3*Δ cells (Fig. 1, left) the bulk of Gap1 (bottom band form) cofractionated with the ER marker Wbp1 (fractions 5 and 6), and there was minimal overlap with the Golgi marker Kex2 (peak fraction 7). Interestingly, a small amount of Gap1 (top band form) cofractionated with Pma1, the PM marker protein (fractions 2 and 3), suggesting that a portion of Gap1 is able to fold independently of Shr3. However, based on our extensive phenotypic analysis of *shr3* mutants, including quantitative amino acid uptake assays, microscopic analysis (indirect immunofluorescence and Gap1-GFP), and biochemical approaches, the fraction of folded and correctly localized Gap1 in *shr3* mutant cells is too low to confer detectable Gap1-dependent phenotypes (Ljungdahl et al., 1992; Kuehn et al., 1996, 1998; Gilstring et al., 1999; Kota and Ljungdahl, 2005). These results demonstrate that Shr3 is required to enable Gap1 to efficiently exit the ER and correctly localize to the PM.

Split Gap1 constructs insert into the membrane and assemble to gain functional conformations in an Shr3-dependent manner

In early studies regarding polytopic membrane protein biogenesis, it was found that truncated N- and C-terminal fragments of bacteriorhodopsin could incorporate into membranes and assemble to attain catalytic active conformations (Huang et al., 1981). Subsequent to this pioneering work, there have been numerous examples of functional "split" polytopic membrane proteins reported in the literature, including bacterial, yeast, and mammalian proteins. To more fully understand the chaperone-dependent folding of AAPs, and to investigate the regions of Gap1 that require Shr3, we sought to take advantage of the possibility that Gap1 could be functionally expressed as a split protein.

The two-dimensional structure of Gap1 is depicted in Fig. 2 A. The N and C termini and even-numbered hydrophilic loops (L2–L10) are oriented toward the cytoplasm. The odd-numbered loops (L1–L11) are luminally oriented during biogenesis and extracellular when Gap1 is correctly localized to the PM. With the exception of L5 (35 amino acids) and L7 (22 amino acids), the odd-numbered loops are short and are composed of <10 amino acids. Consequently, the bulk of the non–membrane-associated amino acids are on the cytoplasmic side of the membrane.

We constructed alleles encoding two matched pairs of N- and C-terminal Gap1 fragments (Fig. 2 B). The first pair, encoded by the *gap1 TM1-5* and *gap1 TM6-12* alleles, expresses nonoverlapping Gap1 fragments truncated between TMS V and VI. The *gap1 TM1-5* allele encodes an N-terminal Gap1 fragment composed of the first 263 amino acid residues, and the *gap1 TM6-12* allele encodes a C-terminal fragment of Gap1 with a methionine residue placed immediately before residues 264–602. The second pair, encoded by the *gap1 TM1-6* and *gap1 TM7-12* alleles, expresses partially overlapping Gap1 fragments truncated between TMS VI and VII. The *gap1 TM1-6* encoded fragment is composed of the N-terminal 320 amino acid residues, and the *gap1 TM7-12* allele has a methionine residue placed before residues 311–602. Each of these alleles is expressed under control of the endogenous *GAP1* promoter.

The truncated Gap1 alleles were separately introduced into the *gap1Δ*-null mutant strain FGY15, and the growth of

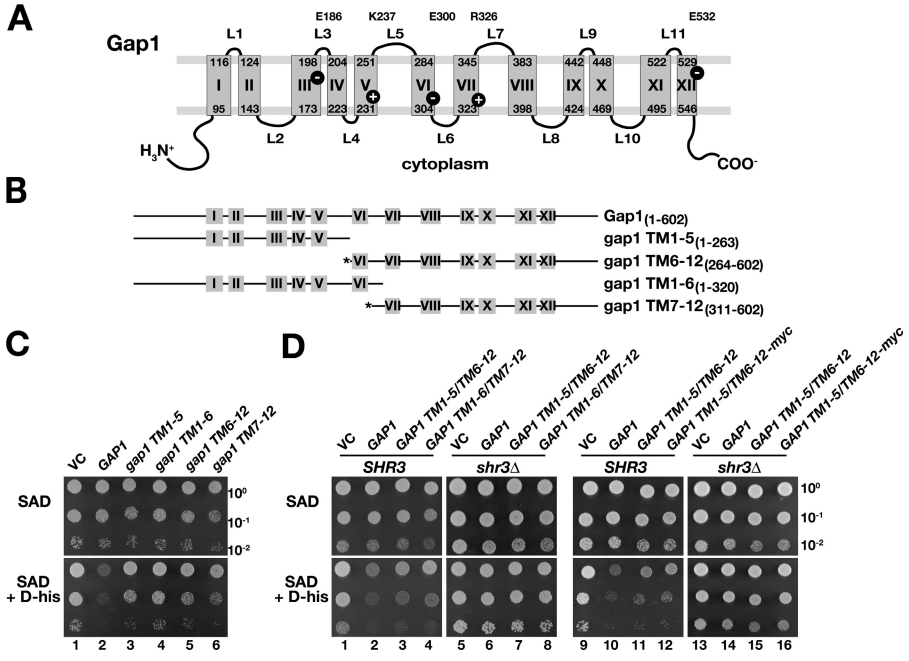

Figure 2. **Gap1 can be split into N- and C-terminal portions that assemble to form a functional permease in an Shr3-dependent manner.** (A) Schematic representation of the membrane topology of Gap1, which is composed of 602 amino acid residues. The gray boxes depict the 12 membrane-spanning segments (I–XII); the numbers within boxes refer to the amino acid residues at the beginning and end of each membrane-spanning segment. The minus and plus symbols represent the positions of the charged amino acid residues in membrane-spanning segments III, V, VI, VII, and XII. (B) Illustration of full-length Gap1 and truncated gap1 constructs. The gray boxes represent the 12 transmembrane segments, the amino acid residues included in each fragment are indicated, and asterisks indicate the insertion of a methionine residue to enable expression of C-terminal fragments. (C) Serial dilutions of cell suspensions of strain FGY15 (*gap1Δ*) carrying vector controls (VC; pRS316 and pRS317), or expressing full-length Gap1 (pPL247 and pRS317) or truncated gap1 constructs were prepared—gap1 TM1-5 (pJK97 and pRS317), gap1 TM1-6 (pJK96 and pRS317), gap1 TM6-12 (pJK99 and pRS316), or gap1 TM7-12 (pJK98 and pRS316), respectively. Aliquots of each dilution were applied to SAD or SAD supplemented with D-histidine (0.15%). (D) Serial dilutions of strain FGY15 (*SHR3 gap1Δ*) or FGY135 (*shr3Δ gap1Δ*) carrying vector controls or expressing full-length Gap1 or coexpressing matched pairs of truncated N- and C-terminal gap1 constructs gap1 TM1-5 (pJK97) and gap1 TM6-12 (pJK99); gap1 TM1-6 (pJK96) and gap1 TM7-12 (pJK98); or gap1 TM1-5 (pJK97) and gap1 TM6-12MYC (pJK100), as indicated, were applied to SAD or SAD with D-histidine (0.15%). Plates were incubated at 30°C for 2.5 d and photographed.

transformants was assessed to determine whether the individually expressed N- and C-terminal fragments exhibited Gap1 transport activity (Fig. 2 C). Gap1 mediates the uptake of toxic D-amino acids (Regenberg and Hansen, 2000); consequently, cells lacking Gap1 activity are able to grow in media containing D-histidine (dilution series 1), whereas cells expressing functional full-length Gap1 cannot (dilution series 2). As expected, cells expressing the truncated N- and C-terminal fragments of Gap1 grew (dilution series 3–6), indicating that the individually expressed truncated proteins are nonfunctional.

Next, plasmids encoding gap1 TM1-5 and gap1 TM6-12 or gap1 TM1-6 and gap1 TM7-12 were introduced together as pairs into FGY15 (*gap1Δ*). The growth of both strains carrying the matched pairs of N- and C-terminal fragments was inhibited by D-histidine (Fig. 2 D; dilution series 3 and 4). All strains grew well in the absence of D-histidine (Fig. 2 D, top); thus, the trivial explanation for the lack of growth, e.g., inhibitory secondary effects resulting from the expression of truncated Gap1 constructs, can be ruled out. These results demonstrate that in both instances, the truncated N- and C-terminal fragments assemble into an active split Gap1 that correctly localizes to the PM and facilitates D-histidine uptake. A slight difference in growth of the split Gap1 expressing strains was noted; the growth of the split Gap1TM1-5/TM6-12 expressing strain (dilution series 3) was nearly as poor as the strain expressing the intact full-length *GAP1* allele (dilution series 2), whereas the growth of the split Gap1TM1-6/TM7-12 expressing strain was better (dilution series 4). The noticeable difference suggests that split Gap1TM1-5/TM6-12 is more active.

To facilitate subsequent biochemical analysis of the C-terminal fragment, we inserted a thrice-reiterated myc epitope immediately preceding the stop codon of the *gap1 TM6-12* allele. We examined the functionality of the C-terminal–tagged split gap1 TM6-12myc construct by coexpressing it with gap1 TM1-5 in strain FGY15 (*gap1Δ*). Growth of this strain (dilution 12) on media containing D-histidine was poor and similar to the untagged Gap1TM1-5/TM6-12 expressing strain (dilution 11). Because growth was inhibited by D-histidine, the myc-tagged split Gap1 was able to assemble together with the N-terminal fragment into an active Gap1.

Finally, we tested whether the untagged and tagged split Gap1 proteins require Shr3 for functional expression (Fig. 2 D; dilution series 5–8 and 13–16, respectively). The matched plasmid pairs were introduced into an *shr3Δ gap1Δ* strain (FGY135). Strain FGY135 is unable to take up D-histidine and grows well because of the lack of Shr3 (dilution series 5 and 13), even when full-length *GAP1* is reintroduced on a plasmid (dilution series 6 and 14). The transformants expressing either of the functional untagged and tagged split Gap1 proteins exhibited robust growth (dilution series 7–8 and 15–16, respectively). The strict requirement for Shr3 indicates that the split proteins, similar to full-length Gap1, require the chaperone activity of Shr3 to attain functional conformations.

Shr3 prevents aggregation of split Gap1

To further investigate the role of Shr3 in Gap1 biogenesis, we examined whether split Gap1TM1-5/TM6-12 and Gap1TM1-5/TM6-12myc aggregate in the absence of Shr3. Cell lysates

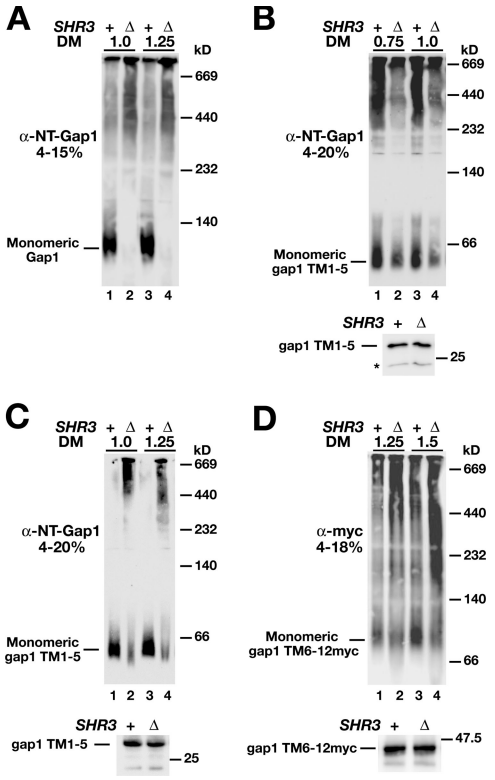

Figure 3. **Shr3 prevents aggregation of assembled split Gap1 constructs.** Extracts from strains FGY15 (*SHR3 gap1Δ*) and FGY135 (*shr3Δ gap1Δ*) expressing full-length Gap1 (pPL247 and pRS317) (A), coexpressing gap1 TM1-5 (pJK97) and gap1 6-12 (pJK99) (B), or coexpressing gap1 TM1-5 (pJK97) and gap1 6-12myc (pJK100) (C and D) were prepared and solubilized with DM at the indicated concentrations (μg DM μg^{-1} protein). Solubilized proteins were separated by BN-PAGE on gradient gels and immunoblotted with anti–NT-Gap1 or c-myc antibodies as indicated. An aliquot of the extracts containing the truncated gap1 constructs (10 μg) was analyzed by SDS-PAGE and immunoblotted with anti–NT-Gap1 (B and C, bottom) or with anti–c-myc antibody (D, bottom). The asterisks indicate a nonspecific immunoreactive band unrelated to Gap1 that fortuitously serves as a loading control.

from strains FGY15 (*gap1Δ*) and FGY135 (*shr3Δ gap1Δ*) expressing full-length Gap1, untagged split Gap1 TM1-5/TM6-12, or tagged Gap1 TM1-5/TM6-12myc were solubilized in the presence of dodecyl-β-D-maltopyranoside (DM), and soluble proteins were separated by blue native PAGE (BN-PAGE; Fig. 3). Consistent with our previous results (Kota and Ljungdahl, 2005), monomeric full-length Gap1 was readily extracted from membranes prepared from *SHR3* wild-type cells (Fig. 3 A, lanes 1 and 3), but not from membranes prepared from *shr3Δ* cells (Fig. 3 A, lanes 2 and 4). In the absence of Shr3, Gap1 aggregates form high molecular weight complexes that migrate as a diffuse smear. Similar results were obtained when we examined untagged split Gap1 (Fig. 3 B); monomers of the N-terminal fragment were readily extracted from membranes containing Shr3 (Fig. 3 B, lanes 1 and 3), whereas fewer monomers were extracted from membranes lacking Shr3 (Fig. 3 B, lanes 2 and 4). We were unable to detect intact assembled split Gap1 monomers, indicating that DM extraction disrupts N- and C-terminal fragment association. The decreased efficiency to solubilize monomeric gap1 TM1-5 in *shr3* mutant cells was not a consequence

of reduced levels of gap1 TM1-5; both *SHR3* and *shr3Δ*strains expressed similar amounts of the N-terminal fragment (Fig. 3 B, bottom).

Antibodies to native Gap1 recognize the N-terminal hydrophilic sequence preceding TMS I (anti-NT-Gap1; De Craene et al., 2001). To investigate the aggregation state of the C-terminal fragment, we coexpressed Gap1 TM1-5/TM6-12myc in *SHR3* and *shr3Δ* cells. In a manner entirely consistent with the untagged split Gap1, the N-terminal fragment was readily extracted from membranes containing Shr3 (Fig. 3 C, lanes 1 and 3), and fewer monomers were extracted from membranes lacking Shr3 (Fig. 3 C, lanes 2 and 4). Next, we assessed whether monomers of the C-terminal fragment could be extracted (Fig. 3 D). Similar to the N-terminal fragment, C-terminal monomers were more readily extracted from membranes with Shr3 (Fig. 3 D, lanes 1 and 3) compared with membranes lacking Shr3 (Fig. 3 D, lanes 2 and 4). However, the difference between gap1 TM6-12myc monomer levels in extracts from *SHR3* and *shr3Δ*cells was not as striking as for the N-terminal fragment. The *SHR3* and *shr3Δ* strains expressed similar amounts of the N- and C-terminal fragments (Fig. 3, C and D, bottom). These results indicate that in the absence of Shr3, the N- and C-terminal fragments of split Gap1 are prone to aggregation.

Shr3 prevents aggregation of individually expressed N-terminal but not C-terminal split Gap1 fragments

To investigate the temporal requirement of Shr3 during the assembly of split Gap, we examined the aggregation state of individually expressed N- and C-terminal fragments. In cells expressing only the N-terminal fragment, gap1 TM1-5 monomers were readily extracted from membranes with Shr3 (Fig. 4 A, lanes 1 and 3), but fewer monomers were extracted from membranes lacking Shr3 (Fig. 4 A, lanes 2 and 4). These results, analogous to what we observe when membranes with coexpressed N- and C-terminal fragments are solubilized (Fig. 3), indicate that Shr3 interacts directly with the N-terminal fragment and prevents its aggregation.

In contrast to the N-terminal fragment, we were unable to find conditions to efficiently extract gap1 TM6-12myc monomers from membranes in cells expressing only the C-terminal fragment (Fig. 4 B). Only small amounts of monomeric gap1 TM6-12myc were extracted, and importantly, the presence (lanes 1 and 3) or absence (lanes 2 and 4) of Shr3 did not affect the levels of soluble C-terminal monomers. These results indicate that in the absence of the first five N-terminal TMSs of Gap1, Shr3 is unable to associate with and prevent aggregation of C-terminal domain of Gap1 containing TMSs VI–XII. The clear Shr3 dependence of the N-terminal fragment is consistent with Shr3 interacting early during the biogenesis of Gap1, an interaction that is likely to occur before the partitioning of all 12 TMSs into the lipid phase of the ER membrane.

Aggregated Gap1 is an ERAD substrate

The observed aggregation of full-length and truncated fragments of Gap1 is the likely consequence of misfolding, which accounts for Gap1 retention and accumulation in the ER of

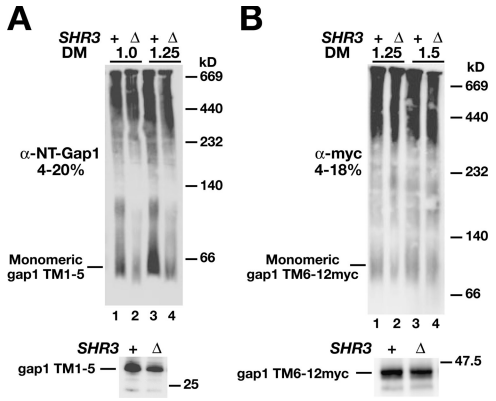

Figure 4. **Temporal requirement of Shr3 in the assembly of split Gap1.** Extracts from strains FGY15 (*SHR3 gap1Δ*) and FGY135 (*shr3Δ gap1Δ*) expressing gap1 TM1-5 (pJK97 and pRS317) (A) or gap1 TM6-12myc (pJK100 and pRS316) (B) were prepared and solubilized with DM at the indicated concentrations (μg DM μg^{-1} protein). Solubilized proteins were separated by BN-PAGE on gradient gels and immunoblotted with anti–NT-Gap1 or c-myc antibodies as indicated. An aliquot of the extracts containing the truncated gap1 constructs (10 μg) were analyzed by SDS-PAGE and immunoblotted with anti–NT-Gap1 (A; bottom) or with anti–c-myc antibody (B; bottom).

shr3Δ mutants. Despite the accumulation of misfolded proteins, *shr3Δ* mutants do not exhibit an activated ER unfolded protein response (Gilstring et al., 1999). This may be explained by the fact that each of the TMSs of Gap1 are correctly inserted in the membrane independently of Shr3 (Gilstring and Ljungdahl, 2000), and that the luminally exposed hydrophilic loops are rather short (Fig. 2 A). Thus, it is likely that Gap1 aggregates do not expose sequences that are recognized by Kar2, the luminal Hsp70 BiP homologue and key regulator of the unfolded protein response (Rutkowski and Kaufman, 2004). Prototrophic *shr3Δ* mutants grow as well as wild-type cells, even under conditions when AAP expression is induced (Ljungdahl et al., 1992), suggesting that *shr3* mutants are not negatively affected by the accumulation of AAP aggregates. To examine how *shr3* mutants cope with AAP aggregates, we examined the turnover of Gap1 using pulse-chase analysis (Fig. 5). Similar to previous reports (Roberg et al., 1997; Gilstring et al., 1999), the half-life of Gap1 in wild-type cells was ∼40 min (Fig. 5, A and C, solid circles). The half-life of Gap1 in *shr3Δ* mutants was similar to wild-type cells (Fig. 5, B and D, solid circles). Thus, despite the fact that Gap1 is differentially localized and present in different forms, i.e., PM and monomeric in *SHR3* versus ER and aggregated in *shr3Δ*, Gap1 is efficiently degraded. The results suggest that AAP aggregates are degraded by ERAD.

To test this possibility, we initially examined the degradation of Gap1 in *pep4Δ* mutants with an impaired capacity to degrade proteins in the vacuole (Jones et al., 1982). In *SHR3* wild-type cells, Gap1 degradation was markedly impaired (Fig. 5 A, open squares), clearly demonstrating that in the presence of Shr3, Gap1 exits the ER and is degraded in the vacuole. This is consistent with the well-characterized trafficking pathways underlying the turnover of PM proteins (Haguenauer-Tsapis and André, 2004). In contrast, Gap1 was efficiently degraded in *shr3Δ pep4Δ* cells (Fig. 5 B, open squares), indicating that Gap1

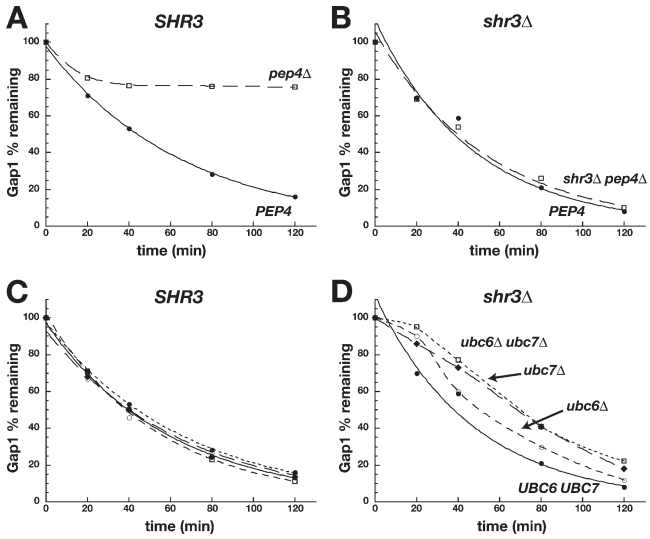

Figure 5. **Gap1 is degraded by ERAD in cells lacking *SHR3*.** Pulse-chase analysis of Gap1 degradation in *SHR3* (A and C) and *shr3Δ*-null mutant cells (B and D). SAD-grown cells were labeled with [^{35}S]methionine for 30 min and chased by the addition of excess unlabeled methionine and cysteine. Aliquots of cells were harvested at times indicated, and Gap1 was immunoprecipitated from cell lysates (see Materials and methods). Immunoprecipitated proteins were separated by SDS-PAGE, and the amount of Gap1-associated radioactivity in samples was quantitated by phosphorimaging. The percentage of radioactivity remaining at each time point from at least two independent experiments is plotted. (A and B) Analysis of Pep4-dependent degradation. In A, solid circles indicate *SHR3* (FGY127) and open squares indicate *pep4Δ* (FGY214). In B, solid circles indicate *shr3Δ* (FGY212) strains and open squares indicate *shr3Δ pep4Δ* (FGY219). (C and D) Analysis of the E2 ubiquitin ligase requirement. Strains in C are indicated as follows: solid circles, *SHR3* (FGY127); open circles, *ubc6Δ* (FGY205); solid diamonds, *ubc7Δ* (FGY206); open squares, *ubc6Δ ubc7Δ* (JKY36). Strains in D are indicated as follows: solid circles, *shr3Δ* (FGY212); open circles, *shr3Δ ubc6Δ* (FGY209); solid diamonds, *shr3Δ ubc7Δ* (FGY210); open squares, *shr3Δ ubc6Δ ubc7Δ* (JKY37).

aggregates are degraded independently of vacuolar hydrolases. This finding is consistent with AAP aggregates being degraded by ERAD.

We examined this directly by constructing *SHR3* and *shr3Δ* strains carrying single- and double-null alleles of the genes encoding ER-localized E2 ubiquitin-conjugating enzymes Ubc6 and Ubc7. Ubc6 and Ubc7 are required for ubiquitylating most characterized luminal and transmembrane ERAD substrates (Meusser et al., 2005). As expected, in *SHR3* cells, the rate of Gap1 degradation was unaffected in *ubc6Δ*, *ubc7Δ*, or *ubc6Δ ubc7Δ* strains (Fig. 5 C). However, in strains lacking Shr3, the rate of Gap1 degradation was diminished in the presence of either *ubc6Δ* or *ubc7Δ* mutations (Fig. 5 D). In comparison to *ubc6Δ*, the *ubc7Δ* mutation exhibited a more pronounced stabilizing affect. Gap1 exhibited the greatest stability in the strain carrying both *ubc6Δ ubc7Δ* mutations. The clear dependency on Ubc6 and Ubc7 demonstrates that aggregated Gap1 is an ERAD substrate.

Doa10- and Hrd1-dependent pathways redundantly target Gap1 for ERAD

Doa10- and Hrd1-dependent ERAD pathways are able to recognize and ubiquitylate membrane protein substrates. However, to date, all characterized ERAD substrates appear to be

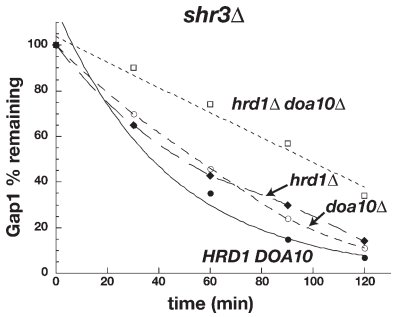

Figure 6. **Doa10- and Hrd1-dependent pathways redundantly target Gap1 aggregates for ERAD in *shr3Δ* mutant cells.** Pulse-chase analysis of Gap1 degradation was performed as in Fig. 4. The percentage of Gap1 remaining in each fraction from two or more independent experiments is plotted. The graph presents an analysis of Doa10- and Hrd1-dependent degradative pathways. Strains are indicated as follows: solid circles, *shr3Δ* (FGY212); open circles, *shr3Δ doa10Δ* (JKY29); solid diamonds, *shr3Δ hrd1Δ* (FGY257); open squares, *shr3Δ hrd1Δ doa10Δ* (JKY39).

preferentially ubiquitylated by either Doa10- or Hrd1-dependent pathways. Thus, these E3 ligases appear to have distinct and nonredundant roles (Ismail and Ng, 2006). To determine which ligase is primarily responsible for ubiquitylating misfolded and aggregated Gap1, we constructed *shr3Δ* strains carrying *doa10Δ*- or *hrd1Δ*-null alleles. Unexpectedly, the stability of Gap1 increased only slightly and to the same extent in both of these strains (Fig. 6). These results suggested that both Doa10- and Hrd1-dependent pathways might function in a redundant manner to ubiquitylate Gap1 aggregates. This possibility was examined by following the degradation of Gap1 in an *shr3Δ* strain carrying both *doa10Δ*- and *hrd1Δ*-null alleles. In this strain, Gap1 was significantly stabilized, indicating that with respect to ubiquitylating Gap1 aggregates, Doa10 and Hrd1 are equally effective and, indeed, functionally redundant. Thus, multiple ERAD pathways are involved in the degradation of Gap1 aggregates.

Agp1 and Gap1 aggregates are degraded similarly

We sought to test whether our findings regarding the turnover of Gap1 can be applied to other AAPs and chose to investigate the turnover of Agp1 (Iraqui et al., 1999). We previously showed that Agp1 aggregates and is retained in the ER of cells lacking Shr3 (Kota and Ljungdahl, 2005). Using a simplified experimental approach relying on cycloheximide, we found that, in wild-type cells, Agp1 is primarily degraded in the vacuole (Fig. 7 A); Agp1 was stabilized in a *pep4Δ* mutant, whereas degradation was unaffected by the combination of *ubc6Δ ubc7Δ* mutations. In cells lacking Shr3, the stability of Agp1 was dependent on ERAD (Fig. 7 B). In these cells, the turnover of Agp1 was largely Pep4 independent and, rather, was Ubc6 and Ubc7 dependent. As was found for Gap1, *ubc7* mutations alone stabilized Agp1 aggregates almost as efficiently as *ubc6 ubc7* double mutations (not depicted). Also, both Doa10- and Hrd1-dependent pathways redundantly targeted Agp1 for degradation; aggregates were degraded in *doa10Δ* and *hrd1Δ* single mutants with equal efficiency but were stable in *doa10Δ hrd1Δ*

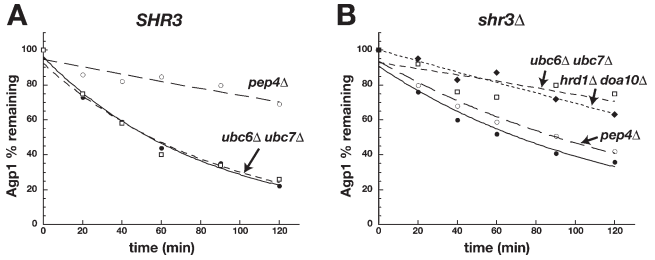

Figure 7. **Agp1 is degraded similar to Gap1 in *shr3Δ* mutant cells.** *SHR3* and *shr3Δ* strains carrying plasmid pJK60 (*STP1Δ131*; Andréasson and Ljungdahl, 2002) to constitutively induce *AGP1* expression were grown in SAD. Cycloheximide was added and lysates were prepared at the times indicated. Proteins, resolved by SDS-PAGE, were analyzed by immunoblotting using polyclonal rabbit anti-Agp1 (1:10,000). Immunoreactive bands were visualized using chemiluminescence detection reagents, and the chemiluminescent signals were quantitated. The percentage of Agp1 remaining in each fraction from two or more independent experiments is plotted. (A) Analysis of Agp1 degradation in *SHR3* cells. Solid circles, *SHR3* (FGY127); open circles, *pep4Δ* (FGY214); open squares, *ubc6Δ ubc7Δ* (JKY36). (B) Analysis of Agp1 degradation in *shr3Δ* cells. Solid circles, *shr3Δ* (FGY212); open circles, *shr3Δ pep4Δ* (FGY219); open squares, *shr3Δ ubc6Δ ubc7Δ* (JKY37); solid diamonds, *shr3Δ hrd1Δ doa10Δ* (JKY39).

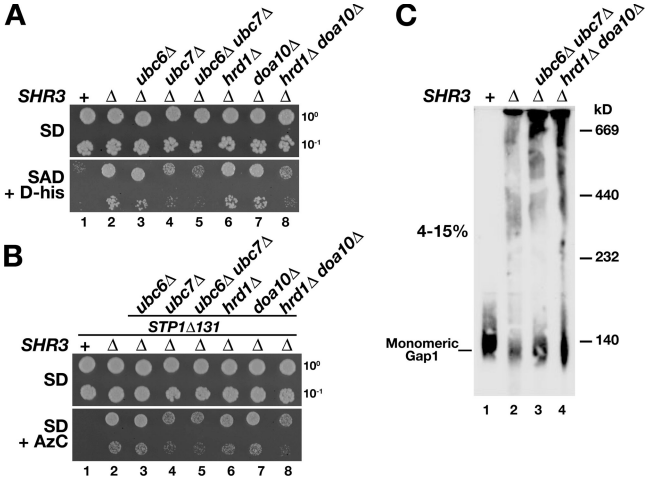

Figure 8. **Mutations that impair ERAD partially suppress *shr3*-null mutant phenotypes.** (A) Growth characteristics of *SHR3* (PLY127), *shr3Δ* (FGY212), *shr3Δ ubc6Δ* (FGY209), *shr3Δ ubc7Δ* (FGY210), *shr3Δ ubc6Δ ubc7Δ* (JKY37), *shr3Δ hrd1Δ* (FGY257), *shr3Δ doa10Δ* (JKY29), and *shr3Δ doa10 hrd1Δ* (JKY39) strains. Cells were resuspended in water to an equal density and 10-fold dilutions were prepared. An aliquot from each dilution was applied to SD SAD containing and D-his (0.15%) to monitor Gap1 activity. (B) Growth of the same strains as in A transformed with pJK60 (*STP1Δ131*) to constitutively induce SPS (Ssy1p-Ptr3p-Ssy5p) sensor–regulated *AGP1* and *GNP1* expression (Andréasson and Ljungdahl, 2002). Aliquots of cell suspensions were applied to SD and SD containing AzC (SD + AzC) to monitor Agp1 and Gnp1 activity (Andréasson et al., 2004). The SD media contained leucine to induce SPS sensor–regulated AAPs. Plates were incubated at 30°C for 3 d and photographed. (C) Extracts from strain PLY127 (*SHR3*), FGY212 (*shr3Δ*), JKY37 (*shr3Δ ubc6Δ ubc7Δ*), and JKY39 (*shr3Δ doa10 hrd1Δ*) grown in SAD were prepared and solubilized with DM (1.25 μg DM μg^{-1} protein). Solubilized proteins were separated by BN-PAGE and immunoblotted with anti–NT-Gap1 antibody.

double mutants. The data demonstrate that Agp1 aggregates are degraded in a manner identical to Gap1 aggregates.

Mutations that compromise ERAD partially suppress *shr3*-null mutant phenotypes

Little is known regarding surveillance mechanisms that monitor the folding of nonglycosylated polytopic membrane proteins, such as AAPs (Gilstring and Ljungdahl, 2000). Although assumed to exist, mechanisms that distinguish between partially folded and misfolded states have not been identified, and the potential role of membrane-localized chaperones in such quality-control mechanisms has not been examined. We suspected that the chaperone activity of Shr3 would have a critical role in discriminating between these two states and perhaps function to shield partially folded AAPs from being prematurely targeted for degradation by ERAD pathways. To evaluate this possibility, we monitored the growth of strains with impaired ERAD using two growth-based assays that provide an extremely sensitive measure of the activity and, hence, the folding state of three AAPs, i.e., Gap1 (Fig. 8 A) and Agp1 and Gnp1 (Fig. 8 B). We reasoned, based on our finding that low levels of Gap1 can apparently fold and exit the ER and reach the PM independently of Shr3 (Fig. 1 B), that if Shr3 normally prevents precocious degradation of AAPs, then mutations that impair ERAD would enable more AAPs to fold properly and lead to increased amino acid uptake.

Consistent with this notion, we observed that in comparison to *shr3Δ* mutants with intact ERAD pathways (Fig. 8; dilution series 2), *shr3Δ* strains carrying mutations that inactivate both Doa10- and Hrd1-dependent ERAD pathways display increased sensitivity to D-histidine and the toxic proline analogue azetidine-2-carboxylate (AzC; Fig. 8; combinations of *ubc6Δ ubc7Δ* or *doa10Δ hrd1Δ*; dilution series 5 and 8, respectively). As observed in our studies analyzing the degradation of Gap1 and Agp1 (Figs. 6 and 7), we noted that strains carrying only the *ubc7Δ* mutation were almost as sensitive to amino acid analogues as the *ubc6Δ ubc7Δ* double mutant strains (Fig. 8; dilution series 4).

The data indicate that under conditions of impaired ERAD, cells have increased levels of properly folded and functional AAPs in their PMs. We tested this possibility directly by examining the aggregation state of Gap1 in the ERAD-defective strains. Membranes from *SHR3*, *shr3Δ*, *shr3Δ ubc6Δ ubc7Δ*, and *shr3Δ doa10 hrd1Δ* strains were solubilized in the presence of DM, and soluble proteins were separated by BN-PAGE (Fig. 8 C). In comparison to membranes from the Shr3 wild-type strain, we observed diminished levels of Gap1 monomers in membranes lacking Shr3 (Fig. 8 C, compare lanes 1 and 2). Substantially more (two- to threefold) Gap1 monomers were extracted from membranes prepared from *shr3Δ* strains carrying *ubc6Δ ubc7Δ* or *doa10 hrd1Δ* mutations (Fig. 8 C, compare lanes 3 and 4 with lane 2). The increased ability to solubilize Gap1 monomers accounts for the increased amino acid uptake in strains with impaired ERAD (Fig. 8, A and B). In summary, our data support the idea that in addition to facilitating folding of AAPs, Shr3 functions to shield partially folded AAPs from being prematurely targeted for degradation.

Discussion

Yeast possesses highly specialized ER membrane-localized chaperones (Kota and Ljungdahl, 2005). In this paper, we have

experimentally addressed two questions regarding the chaperone activity of Shr3. First, is there a temporal requirement for the chaperone activity of Shr3 during the membrane insertion and folding of AAPs? Second, does the chaperone activity of Shr3 affect surveillance mechanisms that monitor the status of membrane protein folding? In answering these questions, we document that Shr3 has a central role in the biogenesis of AAPs, and our results illuminate the tight coupling between folding and quality-control mechanisms operating during biogenesis of polytopic membrane proteins.

We probed the temporal requirement of Shr3 during AAP folding by exploiting the fact that independently coexpressed truncated N- and C-terminal fragments of Gap1 can fold and assemble forming functional split Gap1 proteins (Fig. 2). Importantly, the functional assembly of N- and C-terminal fragments of Gap1 exhibited a strict dependence on Shr3. This finding enabled us to directly analyze whether Shr3 maintains the N- and/or C-terminal fragments in productive assembly competent conformations. Consistent with our previous data regarding full-length Gap1 (Kota and Ljungdahl, 2005), we found that the N-terminal fragment exhibited an increased propensity to aggregate in membranes isolated from cells lacking Shr3, and importantly, its aggregation was not affected by the presence or absence of the C-terminal fragment (Fig. 3, B and C; and Fig. 4 A). In marked contrast, the ability to solubilize monomers of the C-terminal fragment exhibited not only a dependence on Shr3 (Fig. 3 D) but, more significantly, on the presence of the N-terminal fragment (Fig. 4 B). These data are consistent with a model in which Shr3 interacts early during the membrane insertion of AAPs. Furthermore, as the N- and C-terminal fragments are likely to individually insert into the membrane, Shr3 is able to maintain the N-terminal fragment in a conformation that enables the C-terminal fragment to assemble with it. These observations raise many interesting questions regarding how these individual fragments, perhaps in analogy to subunits of multimeric membrane protein complexes, find each other before their functional assembly.

During translocation, exclusively hydrophobic TMSs rapidly partition into the lipid phase of the membrane (Heinrich et al., 2000). In contrast, less hydrophobic TMSs containing charged or polar residues partition into the membrane less readily and are retained in proximity to the translocon or to translocon-associated proteins, e.g., TRAMs (Heinrich and Rapoport, 2003). Recent results regarding the membrane insertion of aquaporin-4 are consistent with the view that individual TMSs exhibit distinct requirements during translocation (Sadlish et al., 2005). After individually passing through a single entry site in Sec61, several TMSs of aquaporin-4 were found to interact with secondary peripheral sites on Sec61. These results suggest that the translocon may transiently retain certain TMSs to facilitate early folding events and to control their release into the membrane (Sadlish et al., 2005). The intrinsic chaperone-like activity of Sec61 translocon may thus suffice to facilitate correct folding of many polytopic membrane proteins.

However, our results regarding membrane-localized chaperones indicate that complex, or larger, polytopic proteins require the assistance of additional chaperones to fold. An appealing hypothesis, consistent with AAP aggregation observed in the absence of Shr3, is that Shr3 facilitates the partitioning of TMSs of AAPs containing charged or polar amino acid residues as they emerge from the translocon. According to this hypothesis, Shr3 may physically shield charged or polar residues within TMSs, enabling them to more rapidly partition into the membrane and fold, thereby preventing them from engaging in nonproductive interactions. Gap1 possesses five TMSs that have a single charged residue (Fig. 2 A). Although we have not systematically investigated the role of these charged residues, in several instances they are conserved, and mutations that exchange noncharged residues into their positions abolish catalytic activity (unpublished data). Consistently, a mutant Gap1 protein with a lysine replacing the conserved glutamate residue (E300) in TMS VI is inactive and retained in the ER (Lauwers and André, 2006).

In cells lacking Shr3, both Gap1 and Agp1 aggregates are efficiently recognized by ERAD surveillance systems that redundantly activate Doa10- and Hrd1-dependent pathways (Figs. 5, 6, and 7). In general, our results are consistent with the recently proposed unifying concept for ERAD (Carvalho et al., 2006). However, to our knowledge, AAP aggregates are the first substrates that target to both Doa10- (ERAD-C) and Hrd1- (ERAD-M/L) dependent pathways with equal efficacy. Our data indicate that these pathways function in parallel to degrade AAP aggregates. However, it is important to note that AAP aggregates may in fact be composed of a nonhomogeneous mix of kinetically linked folding intermediates, which raises the possibility that ERAD pathways preferentially degrade discrete folding intermediates. Previous reports regarding the organization of ERAD pathways suggested that membrane proteins with misfolded cytoplasmic domains are substrates of the Doa10 pathway, whereas soluble secretory proteins and membrane proteins with misfolded luminal or membrane domains are substrates of the Hrd1-dependent pathway (Huyer et al., 2004; Vashist and Ng, 2004; Ismail and Ng, 2006; Ravid et al., 2006). Although it remains to be determined, the involvement of the Doa10 pathway can be explained by the fact that the bulk of the non–membrane-associated amino acids of AAPs are on the cytoplasmic side of the membrane; presumably the folding of cytoplasmic domains are dependent on the proper folding of TMSs. With respect to the Hrd1 pathway, we suspect that in the absence of Shr3, misfolded TMSs of AAPs are recognized. Given the high level of sequence homology and dependence on Shr3, the other members of the AAP protein family are likely to be similarly degraded. Consequently, our findings substantially augment the number of known substrates of the Doa10- and Hrd1-dependent pathways.

We have found that AAPs can attain native structures, albeit inefficiently, independent of the chaperone activity of Shr3 (Figs. 1 and 8). Our finding that mutations that impair ERAD enhance functional expression of AAPs highlights the intimate link between folding and degradation. There are two possible explanations for the ability of AAPs to fold independently of Shr3. First, a small portion of AAPs may fortuitously fold and attain native conformation as they insert in the membrane. In this case, other chaperones present in the ER membrane may

substitute for the lack of Shr3, or the inherent chaperone-like functions associated with the Sec61 translocon may suffice. Alternatively, AAP aggregates may not be solely composed of terminally misfolded proteins. This raises the possibility that low levels of aggregated AAPs are able to reenter a productive folding pathway. Because the topological orientation of each TMS of Gap1 is correctly fixed as they insert into the membrane (Gilstring and Ljungdahl, 2000), AAPs initiate folding at a point that is already quite constrained (Bowie, 2005). Thus, if provided sufficient time (e.g., in cells with impaired ERAD), aggregated AAPs may spontaneously rearrange from a kinetically trapped conformation into their native lower energy conformations.

The idea that Shr3 interacts with TMSs containing charged residues is consistent with it having a role in surveillance mechanisms that monitor folding. Previous work has demonstrated that charged residues within membrane-spanning segments provide key signals for targeting misfolded proteins for ERAD. In the case of unassembled α-subunits of the T cell receptor, which are retained and degraded in the ER, the degradation determinant was mapped to two basic amino acid residues in the TMS (Bonifacino et al., 1990), and the placement of a single charged residue in a TMS of a cell surface protein caused it to be retained and degraded in the ER (Bonifacino et al., 1991). Thus, by shielding charged amino acid residues, Shr3 not only facilitates folding but also prevents incompletely folded AAPs from being targeted for degradation. Furthermore, the fact that Shr3 does not itself exit the ER (Kuehn et al., 1996), and newly synthesized AAPs copurify with Shr3 (Gilstring et al., 1999), suggests that Shr3 retains actively folding AAPs in the ER. Thus, Shr3 may function analogously to the well-characterized N-linked glycosylation-based quality-control system, which provides temporal cues regarding folding of glycoproteins, preventing their premature exit out of the ER and targeting of folding intermediates to ERAD (Helenius and Aebi, 2004).

Our findings underscore the importance of ER membrane-localized chaperones in governing the stability of membrane proteins. In mammalian cells, insulin-induced gene (INSIG) proteins appear to have chaperone-like activity that influences the sterol-dependent degradation of 3-hydroxy-3-methylglutaryl coenzyme A (HMG CoA) reductase and ER retention of Scap (for review see Goldstein et al., 2006). When sterol levels are high, INSIG proteins bind sterol-sensing membrane domains of HMG CoA reductase and Scap. As a consequence of binding, HMG CoA reductase is targeted to ERAD and Scap is prevented from exiting the ER, two events that lead to decreased cholesterol biosynthesis and uptake. In yeast, the INSIG homologues Nsg1 and Nsg2 associate with HMG CoA reductase, facilitating the folding of the sterol-sensing membrane domain and inhibiting Hrd1-dependent degradation (Flury et al., 2005).

Finally, we note striking similarities between the inefficient folding of AAPs in cells lacking Shr3 and the folding of the mammalian Cl^- channel cystic fibrosis transmembrane conductance regulator (CFTR). The folding of native CFTR is inefficient (Ward and Kopito, 1994): only 25% of synthesized CFTR folds properly, and the remaining 75% is degraded by multiple ERAD mechanisms (Younger et al., 2006). The similarities to the situation in yeast suggest that CFTR folding occurs in the absence of dedicated Shr3-like chaperones; consequently, CFTR folding intermediates are more or less constitutively and prematurely targeted for degradation. The ability of small molecules to act as chaperones, and the temperature-dependent characteristics of CFTR folding supports this notion (Denning et al., 1992; Brown et al., 1996; Loo et al., 2005). Also, the folding intermediate that accumulates as a result of the disease-causing ΔF508 mutation is kinetically trapped. Interactions with Hsp90, which are positively and negatively modulated by cochaperones, determine the fate of this misfolded intermediate (Wang et al., 2006). The down-regulation of cochaperone Aha1 enables ΔF508 CFTR to fold, exit the ER, and become functionally expressed in the PM. Presumably, reduced levels of Aha1 circumvent surveillance mechanisms that normally target ΔF508 CFTR for ERAD. It will be interesting to continue to exploit the yeast system described here to dissect out further mechanistic details regarding the quality-control surveillance systems that monitor the folding of polytopic membrane proteins.

Materials and methods

Strains, plasmids, and media

Yeast strains and plasmids are listed in Table I. FGY206 was created by transforming PLY123 with a PstI–BamHI DNA fragment containing *ubc7Δ::LEU2* from pGR172 (Vassal et al., 1992). FGY205 was created by transforming PLY123 with a HindIII–HindIII DNA fragment containing *ubc6Δ::LEU2* from pTX33 (Sommer and Jentsch, 1993). PLY127 was transformed with a EcoRI–XhoI DNA fragment containing *pep4Δ::hisG-URA3-neo-hisG* from pAS173 (provided by A. Sachs, University of California, Berkeley, Berkeley, CA), and a Ura^+ transformant was propagated on medium containing 5-fluoroorotic acid (FOA), resulting in the unmarked *pep4Δ::hisG* strain FGY217. PLY127, FGY205, FGY206, and FGY217 were transformed with a linear EcoRI–SalI DNA fragment containing *shr3Δ5::hisG-URA3-neo-hisG* from pPL288 (Kuehn et al., 1996); Ura^+ transformants were propagated on FOA-containing medium; and strains FGY212, FGY209, FGY210, and FGY219, each carrying the unmarked *shr3Δ6* deletion, were obtained. FGY257 was constructed by transforming FGY212 with a SphI–SalI DNA fragment containing *hrd1::URA3* (Bays et al., 2001). Strains JKY29 and JKY39 were constructed by deleting the entire sequence of *DOA10* in FGY212 and FGY257 with a PCR-amplified *natMX4* cassette (primers F-doa10D and R-doa10D). JKY36 and JKY37 were constructed from FGY205 and FGY209 by deleting the coding sequence of *UBC7* with a PCR-amplified *natMX4* cassette (primers F-ubc7D and R-ubc7D).

Plasmid pJK92 was created by inserting a 3.4-kb SalI–NotI fragment encoding Gap1 from pPL247 into SalI–NotI–restricted pRS317 (Sikorski and Boeke, 1991). Plasmids expressing split Gap1 constructs under the control of the endogenous *GAP1* promoter were created by homologous recombination in yeast. Plasmids pJK97 (*gap1 TM1-5*) and pJK96 (*gap1 TM1-6*) expressing N-terminal fragments of Gap1 were created by introducing Bsu36I–BglII–restricted pPL247 together with primer pairs F:1-5TM/R:1-5TM and F:1-6TM/R:1-6TM, respectively. Plasmids pJK98 (*gap1 TM7-12*) and pJK99 (*gap1 TM6-12*) expressing C-terminal fragments of Gap1 were created by cotransforming BsiWI–BsaBI restricted pJK92 with primer pairs F:7-12TM/R:7-12TM and F:6-12TM/R:6-12 TM, respectively. A thrice-reiterated myc epitope was inserted at the C terminus, immediately before the stop codon, creating plasmid pJK100; 3×myc was PCR amplified from plasmid pPL329 (primers F-Gap1TM6-12–3×MYC/R-Gap1TM6-12–3×MYC) and cotransformed together with SphI–SalI–restricted pJK99.

Standard media, YPD (yeast extract, peptone, dextrose) and SD (synthetic complete), were prepared as described previously (Burke et al., 2000). Ammonium-based synthetic complex (Andréasson and Ljungdahl, 2002) and minimal media containing urea (SUD), proline (SPD), and allantoin (SAD) as the sole nitrogen source were prepared as described previously (Ljungdahl et al., 1992; Kota and Ljungdahl, 2005). Minimal media were supplemented as required. Media were made solid with 2% (wt/vol) bacto Agar (Difco).

Table I. ***S. cerevisiae* strains and plasmids**

Strain or plasmid	Genotype/description	Source or reference
PLY123	*MATα ura3-52 lys2Δ201 leu2-3,112*	Ljungdahl laboratory
PLY127	*MATα ura3-52 lys2Δ201*	Ljungdahl laboratory
FGY212	*MATα ura3-52 lys2Δ201 shr3Δ6*	This work
FGY206	*MATα ura3-52 lys2Δ201 leu2-3,112 ubc7::LEU2*	This work
FGY210	*MATα ura3-52 lys2Δ201 leu2-3,112 ubc7::LEU2 shr3Δ6*	This work
FGY205	*MATα ura3-52 lys2Δ201 leu2-3,112 ubc6::LEU2*	This work
FGY209	*MATα ura3-52 lys2Δ201 leu2-3,112 ubc6::LEU2 shr3Δ6*	This work
FGY217	*MATα ura3-52 lys2Δ201 pep4Δ*	This work
FGY219	*MATα ura3-52 lys2Δ201 pep4Δshr3Δ6*	This work
FGY257	*MATα ura3-52 lys2Δ201 shr3Δ6 hrd1Δ::URA3*	This work
JKY29	*MATα ura3-52 lys2Δ201 shr3Δ6 doa10Δ::natMX4*	This work
JKY36	*MATα ura3-52 lys2Δ201 leu2-3,112 ubc6Δ::LEU2 ubc7Δ::natMX4*	This work
JKY37	*MATα ura3-52 lys2Δ201 leu2-3,112 shr3Δ6 ubc6Δ::LEU2 ubc7Δ::natMX4*	This work
JKY39	*MATα ura3-52 lys2Δ201 shr3Δ6 hrd1::URA3 doa10Δ::natMX4*	This work
FGY15	***MATa*** *ura3-52 lys2Δ201 leu2-3,112 gap1Δ2::LEU2*	Gilstring and Ljungdahl, 2000
FGY135	***MATa*** *ura3-52 lys2Δ201 leu2-3,112 gap1Δ2::LEU2 shr3Δ6*	Gilstring and Ljungdahl, 2000
pPL247	*GAP1* in pRS316 (*URA3*)	Ljungdahl et al., 1992
pJK92	*GAP1* in pRS317 (*LYS2*)	This work
pJK96	*GAP1 TM1-6* in pPL247	This work
pJK97	*GAP1 TM1-5* in pPL247	This work
pJK98	*GAP1 TM7-12* in pJK92	This work
pJK99	*GAP1 TM6-12* in pJK92	This work
pJK100	*GAP1 TM6-12-3xMyc* in pJK92	This work
PJK60	*STP1Δ131* in pRS317	Kota and Ljungdahl, 2005

Subcellular fractionation and immunoblot analysis

Cells were grown overnight in SD to an OD_{600} of 2–3, harvested, washed once in water, and resuspended in SUD to a starting OD_{600} of 0.1. Cells were grown at 30°C and harvested when cultures reached an OD_{600} of 0.8, and protein extracts were prepared and fractionated on 12–60% sucrose gradients essentially as described previously (Egner et al., 1995). 1-ml fractions were collected from the bottom of the gradients using a Fraction Recovery System (Beckman Coulter). Fractions 1 and 2 and 10 and 11 were separately pooled, and proteins from equal aliquots of the nine resulting fractions were concentrated by TCA precipitation. Proteins were separated by SDS-PAGE and blotted onto nitrocellulose membranes.

Immunoblots were incubated as indicated with primary antibody (rabbit polyclonal) in blocking buffer (phosphate-buffered saline and 0.1% Tween 20) diluted as follows: α-Agp1p, 1:10,000; α-Dap2, 1:2,000; α-Gap1, 1:20,000; α-Kex2, 1:1,000; α-Pma1, 1:3,000; α-Shr3p, 1:1,000; α-Wbp1, 1:1,000. Blots were washed three times for 15 min with wash buffer (blocking buffer plus 5% milk) and incubated with horseradish peroxidase–coupled secondary antibody, donkey α-rabbit Ig (GE Healthcare), diluted 1:5,000 in wash buffer. Blots were washed three times for 15 min with wash buffer, and immunoreactive proteins were visualized by chemiluminescence detection reagents (ECL-PLUS Western Blotting Detection System; GE Healthcare) and the LAS1000 camera system (Fuji). The α-Gap1 and α-Agp1 antisera were provided by B. André (Universite Libre de Bruxelles, Brussels, Belgium). The α-Pma1, α-Wbp1, and α-Kex2 antibodies were obtained from C. Slayman (Yale University, New Haven, CT), S. te Heesen (Swiss Federal Institute of Technology, Zürich, Switzerland), and R. Fuller (University of Michigan, Ann Arbor, MIC), respectively.

Pulse-chase analysis

Radiolabeling and immunoprecipitations were conducted essentially as described previously (Silve et al., 1991; Volland et al., 1994). In brief, cells grown in SAD (plus uracil) to an OD_{600} of 0.5–0.8 were used to inoculate fresh SAD (plus uracil) at an OD_{600} of 3. Cultures were incubated for 30 min before the addition of ^{35}S-methionine (25 μCi/OD_{600} cells; GE Healthcare). Cells were labeled for 30 min, after which an aliquot of 100× chase solution (25 mM L-methionine and 25 mM L-cysteine) was added. At the times indicated, 1-ml aliquots of culture were placed in Eppendorf tubes containing 60 μl ice-cold lysis solution (1.85 M NaOH and 7% β-mercaptoethanol), rapidly mixed by rigorous vortexing, and after a 10-min incubation on ice, 60 μl of 50% TCA was added. Precipitated proteins, pelleted by centrifugation for 15 min at 12,000 *g*, were washed once in 60 μl of 1 M Tris, pH 7.5, and solubilized in 0.5% SDS for 10 min at 37°C. Proteins were diluted with TNET buffer (1% Triton X-100, 50 mM Tris, pH 7.4, 150 mM NaCl, and 5 mM EDTA) to a final volume of 0.6 ml. Insoluble material was removed by centrifugation for 30 min at 12,000 *g*. Rabbit anti-Gap1 antibodies were added (1:1,500), and samples, continuously mixed by inversion, were incubated overnight at 4°C. 40 μl of a 12.5% (vol/vol) suspension of protein A–Sepharose CL-4B beads (GE Healthcare) was added to each sample, and incubations were continued for 3 h at 4°C. Immunoprecipitated material was collected by centrifugation and washed three times with TNET buffer and once with TNET without Triton X-100. Precipitated proteins were eluted by incubation for 10 min at 39°C in 2× SDS-PAGE sample buffer. Eluted proteins were separated by SDS-PAGE in a 10% gel. Gels were fixed in glacial acetic acid/methanol/H_2O (10:20:70), rinsed briefly in water, and dried. Radiolabeled proteins were detected and quantified by phosphorimaging (Fujix Bio-Image Analyzer BAS1500; Fuji).

Evaluation of protein stability in the presence of cycloheximide

Cultures grown at 23°C in SAD (plus uracil) to an OD_{600} of 0.8–1 were treated with 400 μg/ml cycloheximide. At the times indicated, 1-ml aliquots were removed to Eppendorf tubes containing 250 μl ice-cold lysis solution (1.85 M NaOH), rapidly mixing by rigorous vortexing, and after a 10-min incubation on ice, 250 μl of 50% TCA was added. Precipitated proteins, pelleted by centrifugation for 15 min at 12,000 *g*, were washed once in 100 μl of 1 M Tris, pH 7.5, and solubilized in 2× SDS-PAGE sample buffer. Proteins were resolved by SDS-PAGE and analyzed by immunoblotting.

BN-PAGE

BN gels and whole cell protein extracts were prepared as previously described (Kota and Ljungdahl, 2005). Protein extracts from cells grown in SAD at 25°C were solubilized at 4°C for 35 min in the presence of DM at the concentrations indicated. Extracts containing full-length Gap1 and split Gap1 fragments were separated using 4–15% and 4–20% gradient gels, respectively. High molecular weight marker proteins (GE Healthcare) were used as standards.

Members of Ljungdahl laboratory are acknowledged for constructive comments. We are indebted to Bruno André for his generous gifts of α-Gap1

and α-Agp1 antisera. We thank Carolyn Slayman, Stephan te Heesen, and Robert Fuller for α-Pma1, α-Wbp1, and α-Kex2 antibodies, respectively.

This work was supported by the Ludwig Institute for Cancer Research and a grant from the European Union (EFFEXPORT project; QLK3-CT-2001-00533).

Submitted: 18 December 2006
Accepted: 23 January 2007

References

Abramson, J., I. Smirnova, V. Kasho, G. Verner, H.R. Kaback, and S. Iwata. 2003. Structure and mechanism of the lactose permease of *Escherichia coli*. *Science.* 310:610–615.

Alder, N.N., and A.E. Johnson. 2004. Cotranslational membrane protein biogenesis at the endoplasmic reticulum. *J. Biol. Chem.* 279:22787–22790.

Andréasson, C., and P.O. Ljungdahl. 2002. Receptor-mediated endoproteolytic activation of two transcription factors in yeast. *Genes Dev.* 16:3158–3172.

Andréasson, C., E.P.A. Neve, and P.O. Ljungdahl. 2004. Four permeases import proline and the toxic proline analogue azetidine-2-carboxylate into yeast. *Yeast.* 21:193–199.

Bays, N.W., R.G. Gardner, L.P. Seelig, C.A. Joazeiro, and R.Y. Hampton. 2001. Hrd1p/Der3p is a membrane-anchored ubiquitin ligase required for ER-associated degradation. *Nat. Cell Biol.* 3:24–29.

Bonifacino, J.S., C.K. Suzuki, and R.D. Klausner. 1990. A peptide sequence confers retention and rapid degradation in the endoplasmic reticulum. *Science.* 247:79–82.

Bonifacino, J.S., P. Cosson, N. Shah, and R.D. Klausner. 1991. Role of potentially charged transmembrane residues in targeting proteins for retention and degradation within the endoplasmic reticulum. *EMBO J.* 10:2783–2793.

Bowie, J.U. 2005. Solving the membrane protein folding problem. *Nature.* 438:581–589.

Brown, C.R., L.Q. Hong-Brown, J. Biwersi, A.S. Verkman, and W.J. Welch. 1996. Chemical chaperones correct the mutant phenotype of the delta F508 cystic fibrosis transmembrane conductance regulator protein. *Cell Stress Chaperones.* 1:117–125.

Bukau, B., J. Weissman, and A. Horwich. 2006. Molecular chaperones and protein quality control. *Cell.* 125:443–451.

Burke, D., D. Dawson, and T. Stearns. 2000. Methods in Yeast Genetics: A Cold Spring Harbor Laboratory Course Manual. Cold Spring Harbor Laboratory Press, Cold Spring Harbor, NY. 205 pp.

Carvalho, P., V. Goder, and T.A. Rapoport. 2006. Distinct ubiquitin-ligase complexes define convergent pathways for the degradation of ER proteins. *Cell.* 126:361–373.

De Craene, J.O., O. Soetens, and B. André. 2001. The Npr1 kinase controls biosynthetic and endocytic sorting of the yeast Gap1 permease. *J. Biol. Chem.* 276:43939–43948.

Denic, V., E.M. Quan, and J.S. Weissman. 2006. A luminal surveillance complex that selects misfolded glycoproteins for ER-associated degradation. *Cell.* 126:349–359.

Denning, G.M., M.P. Anderson, J.F. Amara, J. Marshall, A.E. Smith, and M.J. Welsh. 1992. Processing of mutant cystic fibrosis transmembrane conductance regulator is temperature-sensitive. *Nature.* 358:761–764.

Egner, R., Y. Mahé, R. Pandjaitan, and K. Kuchler. 1995. Endocytosis and vacuolar degradation of the plasma membrane-localized Pdr5 ATP-binding cassette multidrug transporter in *Saccharomyces cerevisiae*. *Mol. Cell. Biol.* 15:5879–5887.

Ellgaard, L., M. Molinari, and A. Helenius. 1999. Setting the standards: quality control in the secretory pathway. *Science.* 286:1882–1888.

Engelman, D.M., Y. Chen, C.N. Chin, A.R. Curran, A.M. Dixon, A.D. Dupuy, A.S. Lee, U. Lehnert, E.E. Matthews, Y.K. Reshetnyak, et al. 2003. Membrane protein folding: beyond the two stage model. *FEBS Lett.* 555:122–125.

Flury, I., R. Garza, A. Shearer, J. Rosen, S. Cronin, and R.Y. Hampton. 2005. INSIG: a broadly conserved transmembrane chaperone for sterol-sensing domain proteins. *EMBO J.* 24:3917–3926.

Gilstring, C.F., and P.O. Ljungdahl. 2000. A method for determining the in vivo topology of yeast polytopic membrane proteins demonstrates that Gap1p fully integrates into the membrane independently of Shr3p. *J. Biol. Chem.* 275:31488–31495.

Gilstring, C.F., M. Melin-Larsson, and P.O. Ljungdahl. 1999. Shr3p mediates specific COPII coatomer-cargo interactions required for the packaging of amino acid permeases into ER-derived transport vesicles. *Mol. Biol. Cell.* 10:3549–3565.

Goldstein, J.L., R.A. DeBose-Boyd, and M.S. Brown. 2006. Protein sensors for membrane sterols. *Cell.* 124:35–46.

Haguenauer-Tsapis, R., and B. André. 2004. Membrane trafficking of yeast transporters: mechanisms and physiological control of downregulation. *In* Topics in Current Genetics—Molecular Mechanisms Controlling Transmembrane Transport. E. Boles and R. Krämer, editors. Springer-Verlag, Heidelberg, Germany. 273–323.

Heinrich, S.U., and T.A. Rapoport. 2003. Cooperation of transmembrane segments during the integration of a double-spanning protein into the ER membrane. *EMBO J.* 22:3654–3663.

Heinrich, S.U., W. Mothes, J. Brunner, and T.A. Rapoport. 2000. The Sec61 complex mediates the integration of a membrane protein by allowing lipid partitioning of the transmembrane domain. *Cell.* 102:233–244.

Helenius, A., and M. Aebi. 2004. Roles of N-linked glycans in the endoplasmic reticulum. *Annu. Rev. Biochem.* 73:1019–1049.

Huang, K.S., H. Bayley, M.J. Liao, E. London, and H.G. Khorana. 1981. Refolding of an integral membrane protein. Denaturation, renaturation, and reconstitution of intact bacteriorhodopsin and two proteolytic fragments. *J. Biol. Chem.* 256:3802–3809.

Huang, Y., M.J. Lemieux, J. Song, M. Auer, and D.N. Wang. 2003. Structure and mechanism of the glycerol-3-phosphate transporter from *Escherichia coli*. *Science.* 301:616–620.

Huyer, G., W.F. Piluek, Z. Fansler, S.G. Kreft, M. Hochstrasser, J.L. Brodsky, and S. Michaelis. 2004. Distinct machinery is required in *Saccharomyces cerevisiae* for the endoplasmic reticulum-associated degradation of a multispanning membrane protein and a soluble luminal protein. *J. Biol. Chem.* 279:38369–38378.

Iraqui, I., S. Vissers, F. Bernard, J.O. de Craene, E. Boles, A. Urrestarazu, and B. André. 1999. Amino acid signaling in *Saccharomyces cerevisiae*: a permease-like sensor of external amino acids and F-Box protein Grr1p are required for transcriptional induction of the *AGP1* gene, which encodes a broad-specificity amino acid permease. *Mol. Cell. Biol.* 19:989–1001.

Ismail, N., and D.T. Ng. 2006. Have you HRD? Understanding ERAD is DOAble! *Cell.* 126:237–239.

Jones, E.W., G.S. Zubenko, and R.R. Parker. 1982. *PEP4* gene function is required for expression of several vacuolar hydrolases in *Saccharomyces cerevisiae*. *Genetics.* 102:665–677.

Kota, J., and P.O. Ljungdahl. 2005. Specialized membrane-localized chaperones prevent aggregation of polytopic proteins in the ER. *J. Cell Biol.* 168:79–88.

Kuehn, M.J., R. Schekman, and P.O. Ljungdahl. 1996. Amino acid permeases require COPII components and the ER resident membrane protein Shr3p for packaging into transport vesicles in vitro. *J. Cell Biol.* 135:585–595.

Kuehn, M.J., J.M. Herrmann, and R. Schekman. 1998. COPII-cargo interactions direct protein sorting into ER-derived transport vesicles. *Nature.* 391:187–190.

Lauwers, E., and B. André. 2006. Association of yeast transporters with detergent-resistant membranes correlates with their cell-surface location. *Traffic.* 7:1045–1059.

Lecomte, F.J., N. Ismail, and S. High. 2003. Making membrane proteins at the mammalian endoplasmic reticulum. *Biochem. Soc. Trans.* 31:1248–1252.

Ljungdahl, P.O., C.J. Gimeno, C.A. Styles, and G.R. Fink. 1992. SHR3: a novel component of the secretory pathway specifically required for the localization of amino acid permeases in yeast. *Cell.* 71:463–478.

Loo, T.W., M.C. Bartlett, and D.M. Clarke. 2005. Rescue of folding defects in ABC transporters using pharmacological chaperones. *J. Bioenerg. Biomembr.* 37:501–507.

Meusser, B., C. Hirsch, E. Jarosch, and T. Sommer. 2005. ERAD: the long road to destruction. *Nat. Cell Biol.* 7:766–772.

Nagamori, S., I.N. Smirnova, and H.R. Kaback. 2004. Role of YidC in folding of polytopic membrane proteins. *J. Cell Biol.* 165:53–62.

Nishikawa, S., J.L. Brodsky, and K. Nakatsukasa. 2005. Roles of molecular chaperones in endoplasmic reticulum (ER) quality control and ER-associated degradation (ERAD). *J. Biochem. (Tokyo).* 137:551–555.

Osborne, A.R., T.A. Rapoport, and B. van den Berg. 2005. Protein translocation by the Sed61/secY channel. *Annu. Rev. Cell Dev. Biol.* 21:529–550.

Popot, J.L., and D.M. Engelman. 1990. Membrane protein folding and oligomerization: the two-stage model. *Biochemistry.* 29:4031–4037.

Rapoport, T.A., V. Goder, S.U. Heinrich, and K.E.S. Matlack. 2004. Membrane-protein integration and the role of the translocation channel. *Trends Cell Biol.* 14:568–575.

Ravid, T., S.G. Kreft, and M. Hochstrasser. 2006. Membrane and soluble substrates of the Doa10 ubiquitin ligase are degraded by distinct pathways. *EMBO J.* 25:533–543.

Regenberg, B., and J. Hansen. 2000. GAP1, a novel selection and counter-selection marker for multiple gene disruptions in *Saccharomyces cerevisiae*. *Yeast.* 16:1111–1119.

Roberg, K.J., N. Rowley, and C.A. Kaiser. 1997. Physiological regulation of membrane protein sorting late in the secretory pathway of *Saccharomyces cerevisiae*. *J. Cell Biol.* 137:1469–1482.

Rutkowski, D.T., and R.J. Kaufman. 2004. A trip to the ER: coping with stress. *Trends Cell Biol.* 14:20–28.

Sadlish, H., D. Pitonzo, A.E. Johnson, and W.R. Skach. 2005. Sequential triage of transmembrane segments by Sec61alpha during biogenesis of a native multispanning membrane protein. *Nat. Struct. Mol. Biol.* 12:870–878.

Sikorski, R.S., and J.D. Boeke. 1991. In vitro mutagenesis and plasmid shuffling: from cloned gene to mutant yeast. *Methods Enzymol.* 194:302–318.

Silve, S., C. Volland, C. Garnier, R. Jund, M.R. Chevallier, and R. Haguenauer-Tsapis. 1991. Membrane insertion of uracil permease, a polytopic yeast plasma membrane protein. *Mol. Cell. Biol.* 11:1114–1124.

Sommer, T., and S. Jentsch. 1993. A protein translocation defect linked to ubiquitin conjugation at the endoplasmic reticulum. *Nature.* 365:176–179.

Springael, J.Y., and B. André. 1998. Nitrogen-regulated ubiquitination of the Gap1 permease of *Saccharomyces cerevisiae*. *Mol. Biol. Cell.* 9:1253–1263.

Stanbrough, M., and B. Magasanik. 1995. Transcriptional and posttranscriptional regulation of the general amino acid permease of *Saccharomyces cerevisiae*. *J. Bacteriol.* 177:94–102.

van den Berg, B., W.M. Clemons Jr., I. Collinson, Y. Modis, E. Hartmann, S.C. Harrison, and T.A. Rapoport. 2004. X-ray structure of a protein-conducting channel. *Nature.* 427:36–44.

Vashist, S., and D.T. Ng. 2004. Misfolded proteins are sorted by a sequential checkpoint mechanism of ER quality control. *J. Cell Biol.* 165:41–52.

Vassal, A., A. Boulet, E. Decoster, and G. Faye. 1992. QRI8, a novel ubiquitin-conjugating enzyme in *Saccharomyces cerevisiae*. *Biochim. Biophys. Acta.* 1132:211–213.

Volland, C., J.M. Galan, D. Urban-Grimal, G. Devilliers, and R. Haguenauer-Tsapis. 1994. Endocytose and degradation of the uracil permease of *S. cerevisiae* under stress conditions: possible role of ubiquitin. *Folia Microbiol. (Praha).* 39:554–557.

Wang, X., J. Venable, P. Lapointe, D.M. Hutt, A.V. Koulov, J. Coppinger, C. Gurkan, W. Kellner, J. Matteson, H. Plutner, et al. 2006. Hsp90 cochaperone Aha1 downregulation rescues misfolding of CFTR in cystic fibrosis. *Cell.* 127:803–815.

Ward, C.L., and R.R. Kopito. 1994. Intracellular turnover of cystic fibrosis transmembrane conductance regulator. Inefficient processing and rapid degradation of wild-type and mutant proteins. *J. Biol. Chem.* 269:25710–25718.

Younger, J.M., L. Chen, H.Y. Ren, M.F. Rosser, E.L. Turnbull, C.Y. Fan, C. Patterson, and D.M. Cyr. 2006. Sequential quality-control checkpoints triage misfolded cystic fibrosis transmembrane conductance regulator. *Cell.* 126:571–582.